

Análise teórica e experimental de lajes pré-fabricadas compostas por vigotas protendidas

Theoretical and experimental analysis of precast slabs composed of pre-stressed joists

Jordan Kasparý¹, Hinoel Zamis Ehrenbring² , Fernanda Pacheco² ,
Roberto Christ^{2,3}, Uziel Cavalcanti de Medeiros Quinino², Bernardo Fonseca Tutikian² 

¹Kasparý Engenharia. R. Domingos de Almeida, 338, Centro, 93510-000, Novo Hamburgo, RS, Brasil.

²Universidade do Vale do Rio dos Sinos, Instituto Tecnológico em desempenho e construção civil (itt Performance). Avenida Unisinos, 950, 93022-750, São Leopoldo, RS, Brasil.

³Universidad de La Costa, Departamento de Engenharia Civil e Ambiental. Calle 58 # 55-66, Barranquilla, Colômbia.

ABSTRACT

The composite precast slabs are composite systems, in which they are constituted by concrete joists (reinforced or prestressed), filling components and a solidarization layer in reinforced concrete. It is a construction system widely used in the world, mainly in Ibero-American countries, such as Brazil and Spain, for example. However, there is still a lack of knowledge about the compatibility between the theoretical results and the experimental ones, since they are composite systems, and the variables can be decisive in the theoretical models. Therefore, this study aimed to compare the theoretical and experimental results of precast composite slabs. This study developed an experimental program of flexing tests for a slab with pre-stressed center joist reinforced on each side with half-longitudinal slab components and a 5 cm mesh-reinforced concrete cover. Experimental variables were the diameter of steel reinforcement and filler material (ceramic blocks or Expanded Polystyrene – EPS blocks). This study has 4 steps: materials characterization, mechanical tests of the joist, effect of filler material in the structural behavior and theoretical and experimental system behavior at fissuring and rupturing. Prestressed joists ruptured in compression regions during bending tests regardless of the diameter of steel reinforcement due to concrete low strength. Filler material did not alter the slabs rupturing load, but EPS blocks allowed considerable deflections. Regarding maximum bending moment, the selected theoretical models had an agreement of up to 99% on experimental values for 4 mm diameter steel-reinforced joists. However, for the joints with 5 and 6 mm wires, the analysis did not prove to be so valid, reaching a ratio of approximately 70 and 60%, respectively.

Keywords: precast slabs; prestressed joists; bending test; maximum bending moment.

RESUMO

Entende-se que as lajes pré-fabricadas mistas são sistemas compostos, nos quais se constituem por vigotas de concreto (armado ou protendido), elementos de preenchimento e uma camada de solidarização em concreto armado. É um sistema construtivo muito utilizado no mundo, principalmente, em países ibero-americanos, como o Brasil e Espanha, por exemplo. No entanto, ainda há desconhecimento sobre a compatibilidade entre os resultados teóricos para os experimentais, uma vez que são sistemas compostos e as variáveis podem ser determinantes nos modelos de previsão. Portanto, este estudo teve como objetivo comparar os resultados teóricos e experimentais de lajes mistas pré-fabricadas. Para isso, desenvolveu um programa experimental de ensaios de flexão para uma laje com vigota central protendida reforçada de cada lado com elementos de laje e uma cobertura de concreto armado com malha de 5 cm. As variáveis experimentais foram o diâmetro da armadura de aço e do material de enchimento (telhas de cerâmica ou blocos de poliestireno expandido). Este estudo tem 4 etapas: caracterização dos materiais, ensaios mecânicos da vigota, efeito do material de enchimento no comportamento estrutural e comportamento teórico e experimental do sistema na fissuração e ruptura. Vigotas protendidas romperam na região de compressão durante os testes de flexão, independentemente do diâmetro da armadura de aço. O material de enchimento não

alterou a carga de ruptura das lajes, mas os blocos de EPS permitiram deflexões consideráveis. Em relação ao momento fletor máximo, os modelos teóricos selecionados apresentaram concordância de até 99% nos valores experimentais para vigotas reforçadas com aço de 4 mm de diâmetro. Entretanto, para as nervuras com fios de 5 e 6 mm, a análise não se mostrou tão válida, chegando a uma relação de aproximadamente, 70 e 60%, respectivamente.

Palavras-chave: lajes pré-fabricadas; vigotas protendidas; ensaio de flexão; momento máximo na flexão.

1. INTRODUCTION

In recent years, the design of floors with large spans has become common in buildings. Implementing these types of floors leads to slabs with high thicknesses, often making the structure uneconomic since part of the structural capacity of this system is used to bear the demands arising from its own weight [1–3]. To solve this problem, joist slabs have been used in place of solid slabs which allows the construction of slabs with greater spans and less weight in the construction system [4]. Joist slabs also simplify design execution, reduce losses, and increase productivity [5,6]. Among these types of slabs, joist slabs made up of precast joists stands out. In addition to the joists, the system consists of filling and concrete elements which can be machined or molded in-situ.

According to Flório [7], the use of precast slabs has increased over the years. This type of construction system is more commonly used in small and medium-sized designs. However, it has also become viable for large projects such as buildings with several floors, buildings with large spans and even bridges. The use of this system is encouraged for low-cost buildings [8].

To solve any country's population housing deficit, celerity in building housing units becomes a necessity. However, it is common for high-rise buildings to have a high cost, given that the land on which they are located represents a large portion of the building added value [9]. According to Cunha [10], simple manufacturing construction systems that include joists without involving expensive or difficult to maintain equipment can present an accessible option for design execution. Due to its outstanding characteristics, such as ease of handling and economy in materials, the use and research of joist slabs has increased.

Guimarães *et al.* [11], in a comparison of the same design conditions of solid and joists slabs, concluded that joist slabs presented the best cost-benefit. Since the use of this construction system is common in the civilian construction market, it is also necessary to validate its quality and safety so that severe unexpected issues such as deflections, deformations and/or excessive cracking are avoided [12]. For example, standard NBR 6118 [13] defines that precast slab must follow the instructions recommended by standard NBR 9062 [14] as well as standard NBR 14859 [15].

According to Flório [7], there has been an increase in research related to joist slab construction systems since it has numerous advantages over solid concrete slabs and other conventional construction systems. Therefore, this study aimed to compare the theoretical and experimental results of precast composite slabs. Thus, it is possible to relate the results obtained by the theoretical models to those obtained in the experimental program, serving as a basis for designers and technical committees of standards.

2. MATERIALS AND METHODS

This study has 4 steps: materials characterization, mechanical tests of the joist with different reinforcement wire diameters, evaluated the effect of filler material in the structural behavior of precast slabs and, finally, theoretical, and experimental system behavior at fissuring and rupturing. this last step conducted tests and theoretical analyses on the best performing precast slabs with prestressed joists with different wire diameters determined in previous step.

The concrete used was of two strength classes: one for the prestressed joists and the other for the concrete cover. Steel wires for active joist reinforcement were considered with diameters of 4 mm, 5 mm and 6 mm. Filler materials were ceramic blocks or Expanded Polystyrene (EPS) blocks. The analysis with ceramic blocks was conducted only for joists with 4 mm wire reinforcement and only for comparison purposes. Section 2.1 through 2.4 present further details of the tests, samples and procedures performed.

2.1. Evaluated the effect of filler material in the behavior of precast slabs

For this analysis, the joist systems were manufactured to represent standard sections of precast slabs. The Figure 1 shows the systems and the dimensions are presented in centimeters. The joist systems were 230 cm long, 47 cm wide and 13 cm high and were composed of a joist, a half filler block on each side and a concrete cover of 5 cm. Steel wires for active joist reinforcement were considered with diameters of 4 mm, 5 mm and 6 mm. It is important to indicate that the two filling materials were placed in the similar dimensions (only the length was different), but with materials of different densities. This influences the weight of the slab. Testing was conducted on 4 samples of each system, which was considered adequate for a comparative analysis.

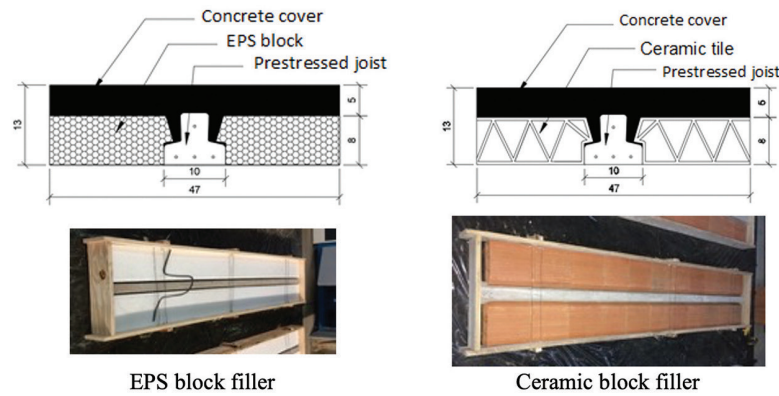


Figure 1: Sample systems of a standard section of a precast slab.

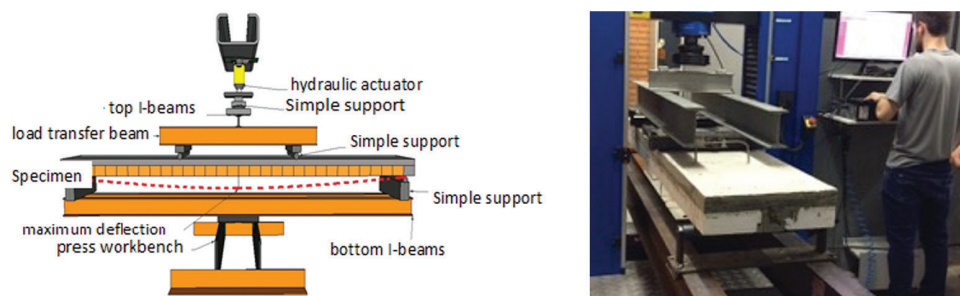


Figure 2: Four-point bending flexural test to determine the mechanical characteristics of the joist systems.

The components of the joist system were demolded, identified, and stored until testing. The systems were manufactured in a single day to reduce the effect of environmental variables. Throughout the day, temperature was measured to vary between 23.0 °C and 24.0 °C while relative humidity varied between 60.0% and 74.8%. The concrete cover was manufactured from concrete with strength class C30. After mixing, each batch of concrete was cast into the molds following the requirements of standard ABNT NBR 5738 [16]. Specimens used for the compression strength characterization of the concrete were molded from each batch into 4 cylindrical samples measuring 100x200 mm. This characterization was conducted after 28 days of curing.

The structural behavior of each joist system was determined with a 4-point flexural test. The same universal testing machine press was used for the control and application of the load as seen in Figure 2. In this case, the load was applied at two points, with pure flexing between the points and a constant bending moment. Two I-beams were used at the top of the load application system to transfer the load from the press to the specimens while two bottom I-beams were used to receive the reactions from the supports since the system was not fixed at its base. The specimens were placed on two articulated supports over the bottom I-beams. For load application on the systems, the third point loading method was used. Bearing blocks were used to ensure that the force applied was perpendicular to the face of the specimens and was applied without eccentricity. In addition to these components, two metal profiles were used as transition beams to transfer the load from the testing machine to the third points of the specimens.

2.2. Characterization of the materials

The characteristics and the mix ratios of the concrete samples of the study are shown in Table 1. Concretes were of classes C35 and C30 for use in joists and concrete cover, respectively, as noted in standards ABNT NBR 6118 [13] and ABNT NBR 8953 [17].

Compressive strength tests followed standard ABNT NBR 5739 [18], modulus of elasticity tests followed standard ABNT NBR 8522[19] and flexural bending tests followed standard ABNT NBR 12142 [20]. The steel used in the manufacture of prestressed joists was of type CP 190 RB. In this research wires with a diameter of 4, 5 and 6 mm were used. This material was delivered in rolls of approximately 2,300 kg and stored in covered warehouses for protection against weather conditions. Characterization of steel behavior under traction followed standard ABNT NBR ISO 6349 [21]. The characteristics of the EPS block were taken from the manufacturer datasheet and are presented in Table 2. The ceramic block used was made of red ceramic with characteristics also presented in Table 2.

Table 1: Concrete mix ratio by mass and w/c ratio.

CONCRETE ELEMENT	f_c CLASS	CEMENT (CP V)	FINE AGGREGATE			COARSE AGGREGATE		w/c RATIO
			FINE	NATURAL	INDUSTRIAL	GRAVEL 0	GRAVEL 1	
Joint	C35	1.00	0.50	1.55	0.35	2.55	–	0.41
Cover	C30	1.00	–	2.68	0.37	1.45	2.00	0.60

Table 2: EPS and ceramic block properties.

MATERIALS	PROPERTIES						
	DENSITY kg/m ³	$f_{c,10\%}$ MPa	SHEAR STRENGTH MPa	FLEXURAL STRENGTH MPa	WIDTH mm	LENGTH mm	HEIGHT mm
EPS block	12.00	0.04	0.03	0.06	370	1000	80
Ceramic block	600.0	6.50	3.00	1.30	370	200	80

Note: $f_{c,10\%}$ is the compression stress at 10% deformation.

2.3. Mechanical properties of the joists

The prestressed joists were manufactured with an “inverted T” cross section out of concrete and four steel wires of the same diameter. The concrete used for the joists was designed with a compressive strength of 35 MPa and Portland type V cement. The joists were manufactured with a molding machine which moves on rails along a 170-meter-long track. After molding, a tarpaulin is placed on the track to prevent water evaporation from the concrete.

Joists time of production was equivalent to 1 day. Ambient temperature and relative humidity were measured along the day with a hygrometer and were found to vary between 19.5 °C to 22.5 °C and 68.3% to 79.7%. After molding, the prestressed steel wires were slackened within the first 36 hours of curing. The joists were cut into 230 cm long segments 48 hours after molding.

In total, 40 prestressed joists were produced from 3 batches of concrete. Specimens were molded to determine the compression and flexing strength of each concrete mixture. The specimens were molded from each batch as follows: 10 cylindrical specimens 100×200 mm for compression strength tests and 2 prismatic specimens of 150×150×500 mm for tension under bending flexural tests as determined in standard ASTM C1609 [22].

Mechanical characteristic tests were performed on the joists after 28 days of curing in accordance with standard ABNT NBR 15522 [23] in a 300 kN universal press. Deflection data were obtained with a linear voltage differential transducer (LVDT) with a precision of 0.001 mm. The LVDT was positioned at the theoretical midpoint of the element, where the largest deflection was expected. The load application system applied a concentrated load at the center of the span in a 3-point bending flexural test. Loading was kept at 80 N/s until the element ruptured.

2.4. Experimental and theoretical analyses

This step determined the structural behavior of the slab sections manufactured with joists with prestressed steel wires of different diameters and with the best filler material determined from previous step. For the tests, four specimens were manufactured for each system for a total of twelve slab sections. Test procedures, environmental conditions and curing ages were the same as indicated in item 2.3. Theoretical analyses were also conducted with theoretical models for comparison purposes.

When designing structures, two criteria must be met: the serviceability limit state (SLS) and the ultimate limit state (ULS). As defined by standard ABNT NBR 8681 [24], ULS is the limit associated with the occurrence of structural failure, which means the collapse of the structure while SLS is related to the performance of the structure, which means the interruption of its normal use [25]. The balance of forces in a typical section of a slab noting that Stages I and II correspond to SLS and Stage III to ULS, with the design of the structures being carried out in the last stage [8]. Initially, to verify the behavior of the joist, it was necessary to determine its geometric characteristics: area, center of gravity and moment of inertia were determined considering the homogeneous concrete section (concrete + steel). These parameters were used to determine the eccentricity of the prestressed reinforcement and the modulus of strength.

Stresses in the prestressing reinforcement were determined from the three stages. The first was the tension in prestressing reinforcement (σ_{pi}) introduced by the prestressing force (P_i). As determined by standard

ABNT NBR 6118 [13], losses from the tensioning process must be added to the tension value. According to Miotto Soares and Hanai [26], losses due to slipping of the wires at anchoring, initial destressing of the reinforcement and initial retraction of the concrete can be estimated at 7%. Therefore, the tension in the prestressing reinforcement due to the prestressing force before the wires are released (σ_{pa}) is taken as $0,93\sigma_{pi}$.

As soon as the prestressing wires are released, an initial tension (σ_{po}) will act on the reinforcement. To calculate this value, the stress in the concrete at the level of the prestressing reinforcement due to force P_a (σ_{cp}) must first be calculated. Once these values are defined, it is possible to calculate the initial stress in the reinforcement considering the loss due to immediate deformation of the concrete (α_p) [27]. Also, ULS for normal loading consists of checking the maximum bending moment (M_u) of the composite section, that being the joist systems in the case of this study. Regarding the reinforcement, the tensile stress in the center of gravity of the wires was determined from Eq. (1) [27]. It should be noted that the different values of design strength (f_{cd}) presented due to the different concretes in the section must be considered. However, the design strength of the concrete that is not compressed does not affect the calculation of Eq. (1) so that:

$$M_u = A_p \cdot f_{pyd} \cdot z_p \quad (1)$$

where: A_p = prestressed reinforcement cross section area; f_{pyd} = design strength of prestressed steel at yield; z_p = lever arm of the acting forces.

Discrepancies may arise between theoretical and experimental results since model input parameters may not necessarily be the same as real data and there are always variances in experimental measurements. This occurs, for example, when the value of z_p is taken from reference works since determining the real coefficient requires complex measurement techniques and, even at that, the measured value may still lack precision.

Shear verification (tangential stresses) of the joists can be performed considering them as beams. However, due to the difficulty in placing transversal reinforcement in components with small heights, this type of verification is not usually performed [8]. Standard ABNT NBR 6118 [13] allows the use of the slab criteria for shearing of the joists if the spacing between the axes of the joists is equal to or less than 65 cm.

For prestressed joist systems, the tension in the bottom fiber at the instant of wire release (σ_1) must be added to the $f_{ct,m}$ value. Standard ABNT NBR 6118 [13] establishes Eq. (2) for the cracking moment:

$$M_r = \frac{f_{ct,m} \cdot I \cdot c}{y_y} \quad (2)$$

where: $f_{ct,m}$ = average tensile strength of the concrete; I_c = moment of inertia of the cross section of the concrete; y_t = distance from the center of gravity to the most stretched fiber.

Since the transversal slab section, steel surface area, material strength and geometric characteristics of the systems are known a priori, the theoretical model is applied in reverse to determine the load limit of the system. Results are the theoretical fissuring and rupturing loads of the precast slabs. The loads in the slabs can be further split into permanent and variable loads. Permanent loads consist of the precast slab weight, which includes filling components and concrete cover. Variable loads, on the other hand, account for the weight of furniture, people, and objects in the use of the slab [28].

3. RESULTS

3.1. Initial evaluation of concrete and system calibration

Table 3 presents average experimental results of direct tension applied to the steel wires used in the joists. Also presented are reference values from the steel supplier and standard ABNT NBR ISO 6349 [21].

Table 3 shows that the mean experimental steel wire yield stress for all wire diameters ($f_{y,med}$) was on average 10% lower than the reference value of 1,900 MPa ($f_{y,ref}$) listed both by the supplier and standard. This variation was larger than the recommended limit of 5% in standard ABNT NBR ISO 6349 [21]. This significant discrepancy between the measured and supplier properties could lead to considerable differences between the theoretical model and experimental results on the structural behavior of the precast joists and slabs. It should be noted that, in this study, the reference standard and supplier stress values were used in the theoretical model to simulate real applications since actual precast composite slabs experimental data are rarely available.

Average experimental rupture stresses ($f_{u,med}$) diverged further by an average of 14% with respect to reference values. This variation was almost triple of the 5% limit established in standard ABNT NBR 6349 [21].

Table 3: Average experimental and reference values for tensile strength of steel wires used in the joists.

\varnothing (mm)	$f_{y,med}$ (MPa)	$f_{y,ref}$ (MPa)	$f_{u,med}$ (MPa)	$f_{u,ref}$ (MPa)	$\epsilon_{u,med}$ (%)	E_{med} (GPa)
4	$1,734.8 \pm 47.3$	1,900	$1,826.3 \pm 16.3$	2,150	0.75 ± 0.04	215.2 ± 12.8
5	$1,782.5 \pm 57.9$		$1,930.4 \pm 88.1$		0.95 ± 0.04	203.9 ± 11.8
6	$1,697.7 \pm 38.5$		$1,813.6 \pm 6.1$		0.81 ± 0.03	202.9 ± 8.6

Note: $f_{y,med}$ – average yield stress; $f_{y,ref}$ – standard yield stress; $f_{u,med}$ – mean failure stress; $f_{u,ref}$ – standard failure stress; $\epsilon_{u,med}$ – mean strain at failure stress; E_{med} – average modulus of elasticity.

Table 4: Mechanical properties for joist and cover of precast slabs after 28 days.

PROPERTY	JOIST				COVER				
	$\varnothing 4$ mm + CER	$\varnothing 4$ mm + EPS	$\varnothing 5$ mm + EPS	$\varnothing 6$ mm + EPS	$\varnothing 4$ mm + CER	$\varnothing 4$ mm + EPS	$\varnothing 5$ mm + EPS	$\varnothing 6$ mm + EPS	
$f_{c,med}$ (MPa)	Exp	36.5 ± 2.1	37.8 ± 1.7	32.9 ± 1.8	38.8 ± 1.3	33.6 ± 0.8	31.0 ± 0.9	29.0 ± 1.5	29.7 ± 1.4
	Theo.	35.0				30.0			
$E_{ci,med}$ (GPa)	Exp	–				32.2	31.7	30,9	30,2
	Theo.	–				30.0			
$f_{ct,m}$ (MPa)	Exp	4.91	4.51	3.87	4.43	–			
	Theo.	3.0				–			

The discrepancies in mechanical properties could be related to the high use of scrap metal in steel manufacture whose properties could vary according to its source [29]. In some cases, scrap might not be properly classified or inspected which allowed the inclusion of low-grade material that affected negatively the properties of the final product. As noted by Almeida [30], improper sorting and inadequate handling of scrap resulted in problems in products produced from recycled material. In addition to the lower than recommended measured values of $f_{y,med}$ and $f_{u,med}$, there were also considerable variations in standard deviation ($\epsilon_{u,med}$) within the same wire diameter. This further reinforced the scrap metal reuse possibility, since steel wire produced from pristine materials tends to have more constant values of stress regardless of wire diameter. On the other hand, average measured modulus of elasticity (E_{med}) had some variation with respect to wire diameter but remained close to the expected reference value of 205 GPa.

Table 4 presents mechanical properties of the joist and cover of precast slabs produced with different wire diameters after 28 days of curing. Concrete cover is applied both on the prestressed joists and on the compression side of the slabs. Values presented are the averaged over the specimens and theoretical predictions.

The mechanical properties of interest in the manufacture of joists are the concrete compression ($f_{c,med}$) and tensile ($f_{ct,m}$) strengths. As shown in Table 4, average measured values of $f_{ct,m}$ for all joists are above the 3.0 MPa theoretical value which, in theory, should result in a higher fissuring bending moment on the systems. As noted by Surdashaan and Rao [31], cementitious matrix tensile strength was related to the size of pores, connectivity between pores and zone interface between aggregates and cement paste. Consequently, variations in the mix ratio could lead to considerable changes in tensile strength as it was highly susceptible to it. As for $f_{c,med}$, Table 4 reports that average measured values are relatively close to the 35 MPa theoretical value. The exceptions are the joists with 5 mm wire diameter reinforcement which is approximately 6% below the limit. As noted by Romero [32], $f_{c,med}$ affected directly the behavior of the joists due to the prestressed reinforcements by increasing the tensile strength but at the same time increasing the compression stress on the opposite side. Thus, prestressed joists could fracture relatively easily under compression if $f_{c,med}$ was below the expected projected value. Further results confirmed that the joist with 5 mm wire diameter reinforcement underperforms with respect to the others.

As Table 4 indicates, the concrete cover of the precast slabs has theoretical compression strength ($f_{c,med}$) and modulus of elasticity ($E_{ci,med}$) of 30 MPa and 30 GPa, respectively. All concrete covers have $E_{ci,med}$ at or above the limit of 30 GPa which ensures a consistent level performance of the system under deformation. Regarding $f_{c,med}$, results are around the 30 MPa limit with the concrete slightly above it and steel wires slightly below it. These variations later affected mechanical and structural behavior test results of the precast slabs since

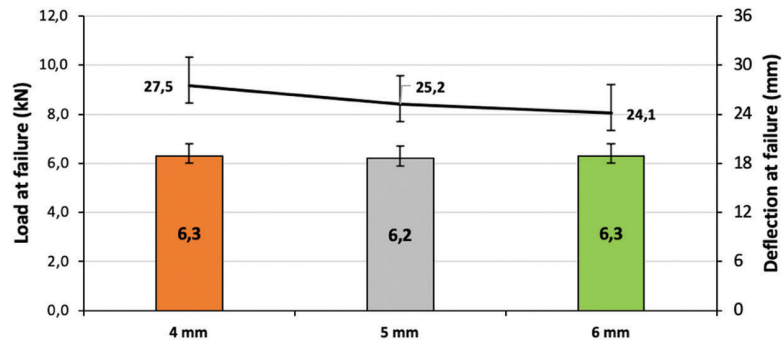


Figure 3: Average values registered at failure of joists: (a) load, (b) deflection.

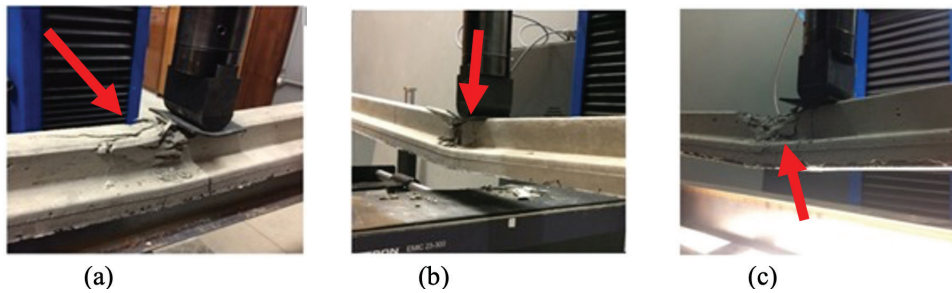


Figure 4: Failure modes of prestressed joists with different steel wires: (a) Ø4 mm, (b) Ø5 mm and (c) Ø6 mm.

input data for the theoretical model differed from measured values. The issue of precise material characterization that can account for the synergy between components (such as strength and adhesiveness) is the main difficulty facing studies that attempt to reconcile computational simulations or theoretical methods to experimental results.

3.2. Mechanical properties of the joists

The results of the for the 3-point flexural bending tests carried out in each batch of joists are presented in Figure 3 as the average values of load at failure and the maximum deflection registered at failure.

As seen in Figure 3, the load applied at failure is similar for all prestressed joists. Increases in steel wire diameter did not increase the load at failure even though it is a commonly attempted technique by manufacturers and project engineers. As a matter of fact, the load at failure was the same for joists with 4 mm and 6 mm diameter wires. This meant that a 125% increase in steel area resulted in no performance gain while increasing production costs. The similarity in behavior of all specimens suggested the failure mode was due to concrete crushing rather than the yield of prestressing wires. Higher maximum loads at failure were expected due to the increase in the diameter of the prestressing wires. In single-axis tension tests of the material, failure loads around 23 kN, 38 kN and 52 kN were recorded for diameters of 4 mm, 5 mm and 6 mm, respectively. However, the crushing of concrete at the top fiber ended up limiting the load-bearing capacity of the joists to around a value of 6 kN for this type of test.

The results of Figure 3 could be attributed to the stress distribution in the transversal section of the joist. Under the 3-point flexural bending test, one side came under tension and the other under compression [33]. Reinforcement increased tensile strength considerably and, as the load increases, overloaded the compression side of the structure. Since concrete strength was at around 35 MPa for all joists, load capacity was also expected to be similar. Consequently, to take advantage of the increased mechanical efficiency brought about by the steel wires, concrete strength must also be increased since it was the main property related to rupturing. This result is confirmed in Figure 4 which shows the rupture of prestressed joists with different steel wire diameters. In all images, it is visually evident that analogous ruptures occurred on the compression region of the joists, because the compressive strength of concrete was the same for all specimens.

With respect to deflection at failure, Figure 3 also shows that the results are similar for the joists but there is a trend of decreased deflection as the diameter of steel wire increased. This result was not necessarily related to the increase in steel cross section but to the joist manufacture. As wire diameter increased, the stress applied during manufacture also increased and resulted in a more prestressed and rigid joist. Since the loads at failure were nearly identical for all joists, the deformation at failure naturally decreased.

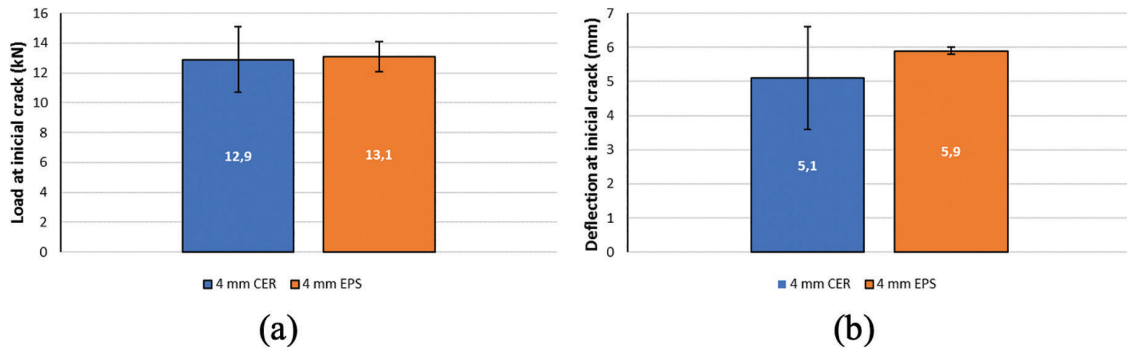


Figure 5: Average values registered at initial appearance of cracks of precast slabs: (a) load, (b) deflection.

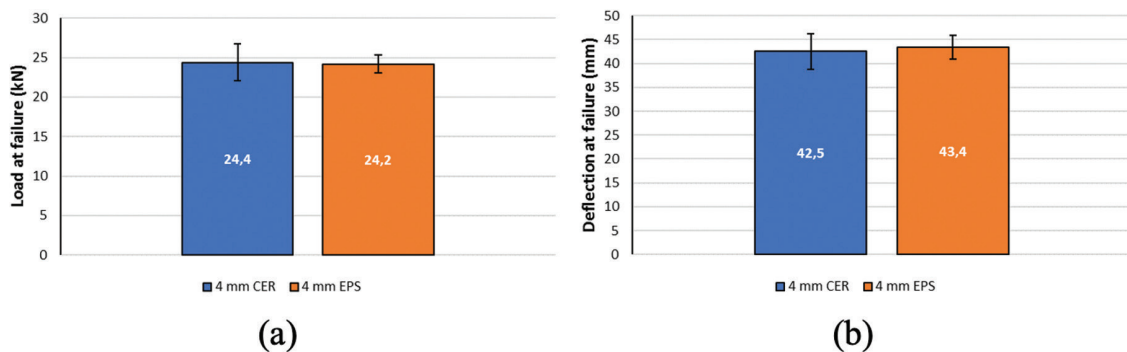


Figure 6: Average values registered at failure of precast slabs: (a) load, (b) deflection.

3.3 Evaluated the effect of filler material in the behavior of precast slabs

Figure 5 present structural behavior results for precast slabs with 4 mm diameter steel wire and ceramic or EPS fillings. The presented average loads and deflections correspond to the serviceability limit state (SLS) reached at the initial appearance of cracks characteristic of fissuring.

Results of Figure 5(a) show that the load at the moment of fissuring is similar, around 13 kN for both slabs. As both precast slabs are the same with only different fillings, this result is extrapolated. However, the standard deviation of the slab with EPS filling is narrower than the one with ceramic blocks. This was likely a result of EPS being an industrialized material with uniform composition which narrowed the response variations of the system [34]. Ceramic blocks, on the other hand, while also industrialized, were also more likely to have a more heterogeneous composition than EPS.

The difference in behavior is more accentuated in deflections at the moment of fissuring. As shown in Figure 5(b) the slab containing EPS deflects more than the one with ceramic blocks. This result was expected since ceramic blocks were a more rigid material with a higher modulus of elasticity which restricted deformations while EPS, with a lower modulus of elasticity allowed larger deformations. This statement is true because the volume fraction of fillers are the same. It should be noted that, despite EPS resulting in a lower strength than ceramic blocks, EPS blocks allowed a reduction in the weight of the system [35].

Figure 6 shows average load and deflection at the moment of failure (rupturing) for precast slabs with 4mm diameter steel wire and ceramic or EPS fillings.

Results of Figure 6 are like the fissuring results of Figure 5. The load at failure is the same 24 kN for both slabs while deflection at failure is nearly the same, with the slab containing EPS deflecting only 2% more than the one with ceramic blocks.

Taken together, the results of Figure 5 and Figure 6 indicate that the main effect of different filling material affected the serviceability limit state (SLS) characterized by fissuring. On the other hand, filing material did not affect the ultimate limit state (ULS) characterized by rupturing. This result was expected since the filling materials were placed in neutral regions of the slab where they were not subjected to loads and, consequently, should not affect the load bearing capacity of the system. However, there were changes to the rigidity of the systems observed as the larger deformation of the less-rigid EPS filled slab. Since the filling materials had similar effects, EPS was selected as the filling material for the remainder of this study to reduce the permanent loads of the system.

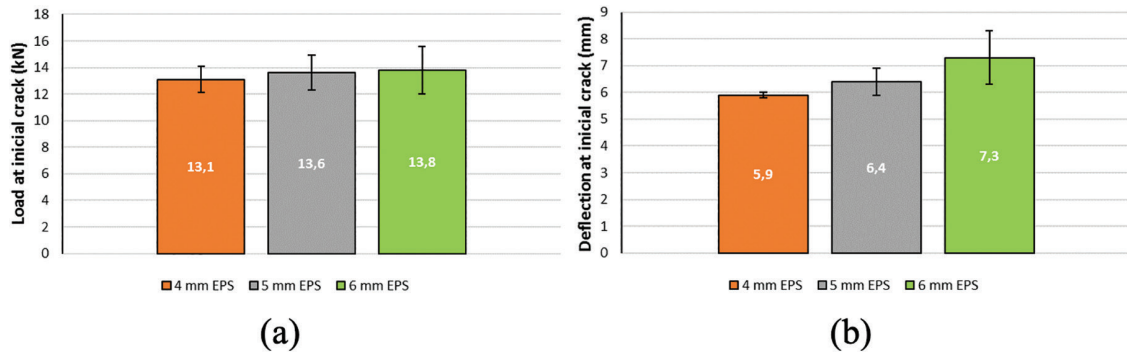


Figure 7: Average values registered at initial cracking of joist systems: (a) load, (b) deflection.

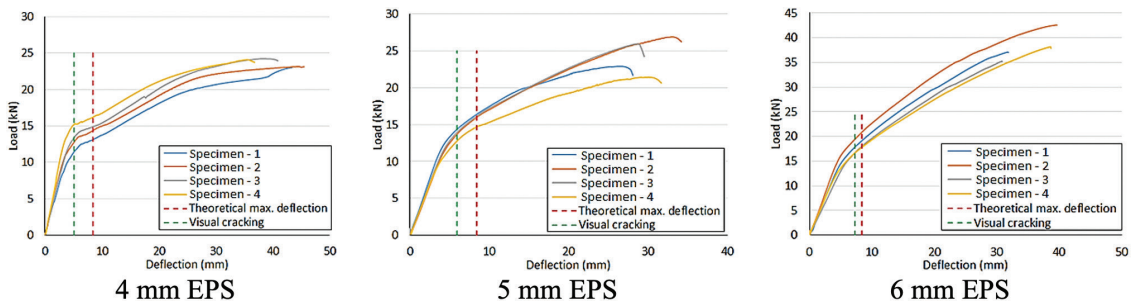


Figure 8: Load vs. deflection curves of joist systems with different wires.

3.4. Experimental Analysis

Figure 7 shows average results related to initial appearance of cracks and corresponding deflection on the joist systems with different steel wire diameters.

Different from the low effect of filling material shown in item 3.3, Figure 8 shows that increases in wire diameter raises slightly the fissuring load of the system from 13 kN to around 14 kN. As noted by Li [36], the initial fissuring load was mainly related to the tensile strength of the concrete used in the joist. As seen in Table 4, $f_{ct,m}$ varied between 3.9 MPa and 4.5 MPa and this variation should have been reflected in the loads at initial cracking if $f_{ct,m}$ was the only factor in determining fissuring. However, it was more likely that pretensioning effects, which were proportional to wire diameter, were the dominant factor in this case. Thus, increased wire diameter resulted in an increase in resistance to fissuring in the joists due to the balancing factors of pretensioning (compression), concrete $f_{ct,m}$ and the loads applied by the bending flexural test.

Similar to the deflections observed in Figure 6b, deflection at fissuring of the joists also increased with increasing wire diameter. The joist with 6 mm diameter wire presented the most gain in resistance to fissuring when compared to smaller diameters. This was evident by the higher load and deflection achieved by the 6 mm wire and EPS filling joist for initial cracks to appear. Thus, an increase in wire diameter increased the SLS for this type of premanufactured slab.

The load-deflection curves applied to the specimens are presented in Figure 8. As in previous results, the average load at initial cracking remained between 13 kN and 14 kN. The initial moment of fissuring occurred at an inflection point in the load curve where the linear SLS behavior became non-linear. This change from linear to non-linear behavior was expected as it had been previously observed by Callister Junior and Rethwisch [37]. The moment of crack initiation occurred immediately after the end of the linear behavior (Stage I of the diagram) indicating the probable beginning of Stage II. In Stage II, only the steel resisted tensile stresses as the concrete cracked at the bottom fiber. However, the uncracked concrete at the top fiber still resisted compressive stresses and retained some linearity.

Analyzing Figure 8, crack initiation occurred for all specimens at a deflection value lower than the value corresponding to the maximum deflection recommended by standard ABNT NBR 6118 [13], which is $L/250$ for L the theoretical span length.

It can be observed in Figure 9 that the maximum load acting on the joist system is higher than the load needed for the steel wire to yield. Steel reaches its yield at a load of approximately 23 kN, which is a value close to the load at failure of most of the specimens. However, the joist systems with 5 mm and 6 mm diameter

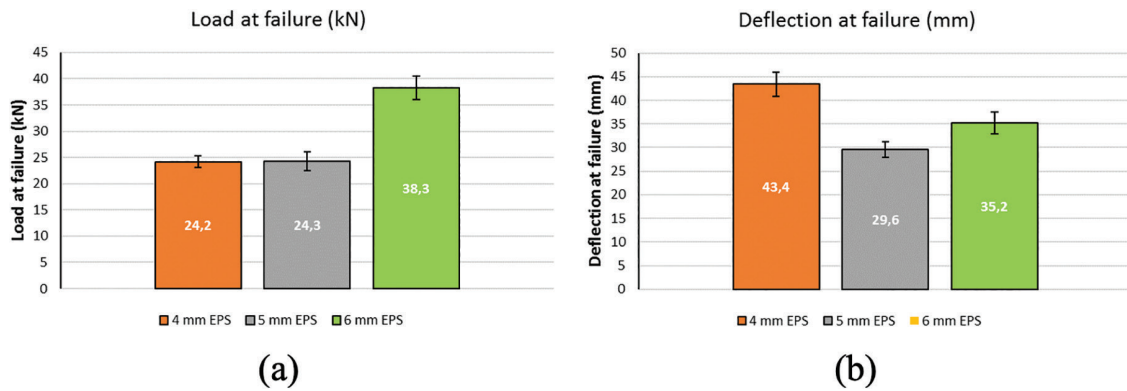


Figure 9: Average values registered at failure of joist systems: (a) load, (b) deflection.

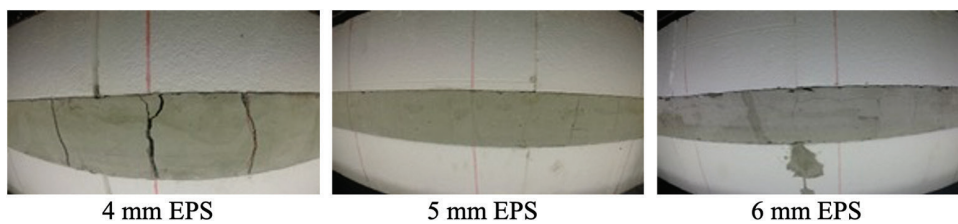


Figure 10: Cracking pattern of joist systems.

wires with EPS filling registered failure at loads below the yield strength of the steel. This result demonstrated a more fragile failure of these specimens characterized by concrete crushing. Standard ABNT NBR 6118 [13] considered the components that fail by compression of the concrete before steel starts to yield as over-reinforced sections. It was concluded that in this situation the maximum capacity of the steel was not reached.

Regarding the joist system with 4 mm diameter wire and EPS filling, Figure 9 shows a similar behavior but with three well-characterized stages. Until the appearance of the first crack, there was a predominant elastic behavior of the material (stage I). Stage I consisted of the initial part of the curve until the appearance of the first cracks (vertical line). As the load increased, the first cracks appeared and started to propagate, representing the cracking stage of the diagram (stage II) and the beginning of compression plasticization. The beginning of stage II could be identified by the change in the slope of the curve while the beginning of stage III could not be observed due to the fragile behavior of concrete under compression. The start of compression plasticization of the concrete (concrete crushing) was denoted by a rapid increase in deflection and could be observed at a load of approximately 24 kN. This indicated stage III occurred from that moment and onwards. Stage III was characterized by the active bending moment approaching the maximum bending moment. Regarding the other two joist systems with 5 and 6 mm wire diameters and EPS filling, only two different stages could be seen in Figure 9.

Overall, it could be concluded that the load-deflection curves of Figure 9 were similar across all specimens and showed a consistent behavior of each particular system. However, the rupture load had considerable variations between specimens which was to be expected in composite systems. The average loads and deflections at failure are shown in Figure 10.

Similar to fissuring results, an increase in transversal area of steel also increased the strength of the joist system. However, Figure 10 shows that, for the 6 mm wire, the increase was more pronounced: a 58% increase in load at failure compared to a 5% increase in load at initial cracking. This increase in load at failure could be explained by the increase in transversal area of steel but, as seen in Figure 4, the overall improvements in joist mechanical properties were not as considerable and the overall benefit might not be worth the increase in production cost. Additionally, going from a 4 mm to a 6 mm diameter wire, the 125% increase in steel transversal area did not result in a proportional structural improvement. This result was not surprising since the composite nature of the system affected the final behavior. Factors such as the strengths of the joist interface with the EPS block or the concrete cover with the EPS block prevented the system from reacting uniformly. Fisher [38] pointed out that to increase the load capacity of a system, techniques such as load redistribution, redesign or reinforcement of joists and the latter could not be obtained simply by increasing the area of steel.

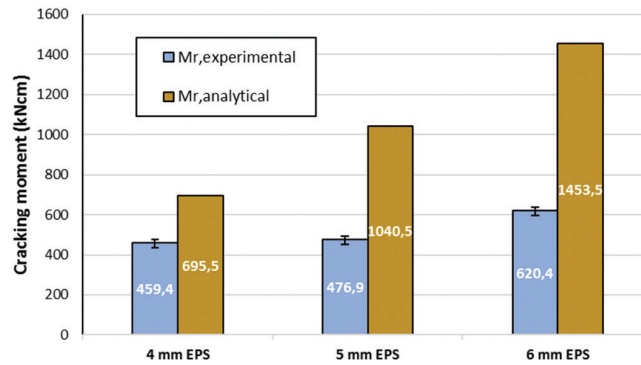


Figure 11: Comparison between experimental and theoretical moment at initial cracking.

Regarding deflection at failure, Figure 9 shows an inverse trend with respect to deflection at initial cracking, that is, larger diameters resulting in lower deflection at failure. This behavior could also be explained by the combined joist strength. As wire diameter increased, so did the strength of the system and its rigidity, decreasing deflection. As the system became more rigid, action and reaction responses were faster and the system ruptured at a lower deflection. This is supported by Figure 8, where the 6 mm diameter specimens had steeper curves characteristic of a more rigid system while the 4 mm diameter ones had shallower curves due to lower strength.

The resulting cracking patterns from the failure of the joist systems are shown in Figure 10. The fissuring aspect was distinct between each system. The joist with 4 mm wire had wider cracks than the others, which correlated with the increase in deflection at failure. In the 5 mm and 6 mm wire joists, the orientation of the cracks was similar but the opening themselves were almost imperceptible. The smallest cracks were observed for the 5 mm wire joist, which also deflected the least. The average spacing between cracks for the 4 mm wire joist was of 5 cm and was related to the deformability of the system. The other systems had less and more spaced fissuring at an average of 15 cm which was characteristic of a higher rigidity.

Failure occurred in the middle third of the span, indicating that the behavior had not changed significantly by using different filling materials. However, the 5 mm wire diameter joist system with EPS filling showed smaller cracks and the failure occurred outside the middle third of the span. This happens when there is some variation in the composition of the specimen. In this way, increasing the opening of few cracks and keeping others thinner. In the other samples, the crack thickness remained constant throughout the element.

Finally, in some 6 mm wire diameter specimens with EPS filling, cracks occurred in the longitudinal direction and the failure point was also outside the middle third of the span. Regarding the failure mode of the 5 mm and 6 mm wire joist systems, the fragile behavior of the concrete cover was the determining factor in the failure of these specimens, as seen from the load-deflection curves shown in Figure 9. The lack of a stage III portion of the curves was also another indicator of weakness in these systems.

3.5. Comparison between theoretical and experimental results

Figure 11 shows the comparison between the theoretical moment required to initiate cracking and the corresponding moment registered in the tests. As seen in the Figure 11, experimental and theoretical cracking moments are different: as the diameter of the steel wire increases, the theoretical moment increases significantly more than the experimental moment.

Figure 11 shows that the differences between the theoretical and experimental moments at fissuring (M_r) can be as high as 134%. It should be noted that no factors of safety were considered in the theoretical models to reflect a more practical behavior. These results contradicted the recommended wisdom that theoretical results should be lower than real results to have a margin of safety. In this case, the minimum structural safety coefficient to ensure a serviceability limit state was 2.34.

Results could be attributed to the variation in $f_{ct,m}$ of the concrete mixtures and the moment of inertia of the composite system. Known theoretical methods are based in homogeneous reinforced sections. For such methods to be applied to this study, the heterogeneous slab with joists and EPS blocks were artificially made homogeneous. This might have resulted in a loss in precision in the theoretical results. Another factor could be related to the y_t variable of the slab, which is the distance from the center of gravity to the most stretched fiber. As the steel wire diameter and transversal area increased, the compression region also increased and y_t tended to decrease. This results in a theoretical increase in cracking moment as seen in Figure 12 which did not occur

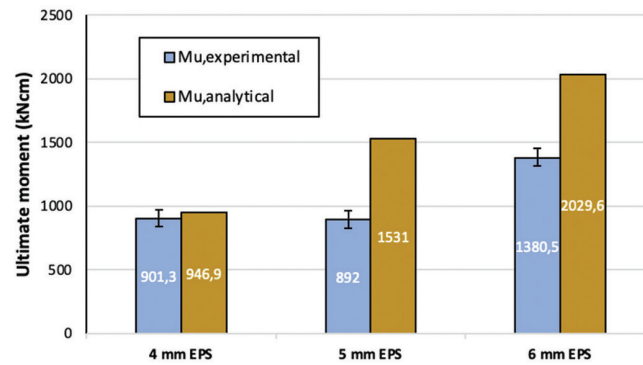


Figure 12: Comparison between the maximum experimental and theoretical moment.

experimentally due to mutual interference of the concrete cover, filling, and joist of the composite slab. Thus, revisions must be sought to the conventional theory used to determine cracking moment.

Figure 12 shows the comparison between the theoretical moment and the registered corresponding experimental moment at failure of the specimens in the tests.

For the 4 mm wire joist systems with EPS filling, the maximum bending moments obtained experimentally were close to the theoretical predictions with differences of only 5% and 6% respectively. In the case of the 5 mm wire joist system, the experimental values corresponded to approximately 58% of the theoretical maximum bending moment. One of the causes of this significant difference between theoretical and experimental results might be related to possible slippage of the active reinforcement due to the adherent prestressing system that was used. However, no such occurrence was observed after examining the specimens. Regarding the 6 mm wire joist system, the maximum experimental bending moment corresponded to approximately 68% of the theoretical moment, which was also a significant difference. In this case, longitudinal cracks were found in the tension region of the joist.

It should be noted that the theoretical method used to calculate the maximum bending moment (M_u) considered the prestressed reinforcement cross section area, design strength of prestressed steel at yield and lever arm of the acting forces. Consequently, the large differences between theoretical and experimental results could be related to the lever arm of the acting forces (z_p) used in the calculations. The actual value of z_p was not measured due to difficulties in installing sensors specific for this variable and the values used were taken from references. Like the fissuring comparison, no factors of safety were considered in the theoretical calculations. Considering the variations obtained in this study, a higher convergence between theoretical and experimental results might be possible with simulation methods such as finite element (FEM).

4. CONCLUSION

Regarding the joists with different wire diameters (4 mm, 5 mm and 6 mm), a similar behavior was observed in terms of cracking pattern, deflections and loads at failure. The failure of the specimens was due to the crushing of the concrete at the top fiber of the joist. The deflections of the joists were similar up to stage I, when the concrete under tension did not yet show crack formation and the load-deflection curve indicated a linear regime before the first crack. With the beginning of cracking and the loss of stiffness (stage II), as expected, the slab systems showed greater deflections.

Considering wire diameters, there was little influence on the performance of prestressed joists. For slab systems, on the other hand, the configuration with 6 mm wire diameter performed better than the other configurations with regards to load-bearing capacity. The slab system with 6 mm wire was more efficient, achieving loads at failure approximately 30% greater and deflections 23% smaller than the slab systems with 4 mm and ceramic filling and 75% smaller than those with 4 mm wire and EPS filling.

Concerning the slab systems, it was determined that failure for the specimens with 4 mm wire was due to yield of the tensile reinforcement. However, for the specimens with 5 mm and 6 mm wires, the loads registered at failure were lower than the loads required to cause the yield of the steel, leading to a fragile failure. These last specimens had EPS filling.

Regarding the filling element used for the slab systems (ceramic or EPS), no significant difference with respect to the maximum bending moments were observed for the specimens with 4 mm wire. The main difference was in the deflection at failure with the specimens with EPS filling registering deflections 50% larger than the specimens with ceramic filling. However, in terms of the load required to reach the deflection limit of $L/250$ set by standard NBR 6118

[13], the values were similar for both systems. This deflection limit was calculated as 8.4 mm and was reached in stage II for all specimens. It can be concluded that the performance of the slab system with EPS filling was similar to the system with ceramic filling, with the advantage of a considerable reduction in weight (about 20%).

By comparing the maximum theoretical bending moment with the experimental one, it was observed that the values were close for the specimens with 4 mm wire regardless of the type of filling type. This indicated that the theoretical model was a good approximation of real behavior. However, for the other specimens, the experimental values were different: about 40% lower for the specimens with 5 mm wire and 30% lower for specimens with the 6 mm wire. Although due care was taken to reproduce the effects of a full-scale model in a reduced system, the difference in the results suggested that each diameter be analyzed separately.

5. REFERENCES

- [1] BROWN, N.C., MUELLER, C., “Design for structural and energy performance of long span buildings using geometric multi-objective optimization”, *Energy and Building*, v. 127, pp. 748–761, 2016. DOI: <http://dx.doi.org/10.1016/j.enbuild.2016.05.090>.
- [2] DROPPA JUNIOR, A., “*Structural analysis of slabs formed by precast elements such as joist with lattice frame*”, M.Sc Thesis, Escola de Engenharia de São Carlos, Universidade de São Paulo, São Carlos, Brasil, 1999.
- [3] SILVA, B.R., “*Contribution to the structural analysis of precast slabs with lattice joists*”, M.Sc Thesis, Universidade Federal de Santa Maria, Santa Maria, Brasil, 2012.
- [4] SARTORI, A.L., FONTES, A.C., PINHEIRO, L.M., “Analysis of the assembling phase of lattice slabs”, *Ibracon Structures and Materials Journal*, v. 6, n. 4, pp. 623–660, 2013. DOI: <https://doi.org/10.1590/S1983-41952013000400008>
- [5] PINHEIRO, L.M., REZANTE, J.A., “Ribbed slabs”, In: *Concrete Structures*. São Carlos, Brasil: Escola de Engenharia de São Carlos, Universidade de São Paulo, 2003.
- [6] SILVA, M.G., “*Comparative study between structural systems of massive and ribbed slabs casted in-situ in a commercial building*”, M.Sc Thesis, Escola de Engenharia de São Carlos, Universidade de São Paulo, São Carlos, 2019.
- [7] FLÓRIO, M.C., *Design and execution of unidirectional slabs with reinforced concrete joists*, São Carlos, Brasil, Universidade Federal de São Carlos, 2004.
- [8] CARVALHO, R.C., FIGUEIREDO FILHO, J.R., *Calculation and detailing of usual reinforced concrete structures*, São Paulo, Brasil, EdUFSCar, 2014.
- [9] CARVALHO, R.C., PINHEIRO, L.M., *Cálculo e detalhamento de estruturas usuais de concreto armado*, São Paulo, PINI, 2009.
- [10] CUNHA, M.O., *Recommendations for the design of slabs formed by joists with lattice frames*, São Carlos, Brasil, Escola de Engenharia de São Carlos, Universidade de São Paulo, 2012.
- [11] GUIMARÃES, M. S., SILVA, C. R., SILVA, J. R., *et al.*, “Comparison of the use of different types of slabs in a reinforced concrete building”, *Revista Mirante*, v. 10, n. 1, pp. 1–20, 2017.
- [12] SANTOS, A.P., *Structural analysis of precast concrete frames*, São Carlos, Brasil, Escola de Engenharia de São Carlos, Universidade de São Paulo, 2010.
- [13] ASSOCIAÇÃO BRASILEIRA DE NORMAS TÉCNICAS, *ABNT NBR 6118: Design of concrete structures — Procedure*, Rio de Janeiro, Brasil, ABNT, 2014.
- [14] ASSOCIAÇÃO BRASILEIRA DE NORMAS TÉCNICAS, *ABNT NBR 9062: Design and execution of precast concrete structures*, Rio de Janeiro, Brasil, ABNT, 2017b.
- [15] ASSOCIAÇÃO BRASILEIRA DE NORMAS TÉCNICAS, *ABNT NBR 14859-1: Pre-fabricated concrete slabs Part 1: Joist, mini-panels and panels – Requirements*, Rio de Janeiro, Brasil, ABNT, 2016a.
- [16] ASSOCIAÇÃO BRASILEIRA DE NORMAS TÉCNICAS, *ABNT NBR 5738: Concrete - Procedure for molding and curing concrete test specimens*. Rio de Janeiro, Brasil, ABNT, 2016b.
- [17] ASSOCIAÇÃO BRASILEIRA DE NORMAS TÉCNICAS, *ABNT NBR 8953: Concrete for structural purposes*, Rio de Janeiro, Brasil, ABNT, 2015.
- [18] ASSOCIAÇÃO BRASILEIRA DE NORMAS TÉCNICAS, *ABNT NBR 5739: Concrete - Compression test of cylindrical specimens*, Rio de Janeiro, Brasil, ABNT, 2018.
- [19] ASSOCIAÇÃO BRASILEIRA DE NORMAS TÉCNICAS, *ABNT NBR 8522: Concrete - Determination of static modulus of elasticity and deformation by compression*, Rio de Janeiro, Brasil, ABNT, 2017a.

- [20] ASSOCIAÇÃO BRASILEIRA DE NORMAS TÉCNICAS, *ABNT NBR 12142: Concrete - Determination of tension strength in flexure of prismatic specimens*. Rio de Janeiro, Brasil, ABNT, 2010.
- [21] ASSOCIAÇÃO BRASILEIRA DE NORMAS TÉCNICAS, *ABNT NBR 6349: Steel wire, bar and strand for reinforcement of prestressed concrete - Tension test*. Rio de Janeiro, Brasil, ABNT, 2008.
- [22] AMERICAN SOCIETY FOR TESTING AND MATERIALS, *ASTM C1609/C1609M-19a, Standard Test Method for Flexural Performance of Fiber-Reinforced Concrete (Using Beam With Third-Point Loading)*, West Conshohocken, PA, ASTM International, 2019.
- [23] ASSOCIAÇÃO BRASILEIRA DE NORMAS TÉCNICAS, *ABNT NBR 15522: Precast slabs - Performance evaluation of ribs and precast plank composite slabs under load*, Rio de Janeiro, Brasil, ABNT, 2007.
- [24] ASSOCIAÇÃO BRASILEIRA DE NORMAS TÉCNICAS, *ABNT NBR 8681: Actions and safety of structures – Procedure*, Rio de Janeiro, Brasil, 2004.
- [25] SALES, J.J., MUNAIAR NETO, J., MALITE, M., *Structural safety*, Rio de Janeiro, Brasil, Elsevier, 2015.
- [26] MIOTTO SOARES, A.M., HANAI, J.B., “Structural analysis of plan frames of precast concrete elements considering the deformability of the connections.”, *Cadernos de Engenharia de Estruturas*, v. 17, pp. 29–57, 2001.
- [27] MERLIN, A.J., *Negative bending moments in slab supports formed by prestressed concrete beams*, Escola de Engenharia de São Carlos, Universidade de São Paulo, São Carlos, Brasil, 2002.
- [28] SCHNEIDER, D., “*Scaling of unidirectional precast ribbed slabs*”, Monograph (Bachelor of Civil Engineering), University of Vale do Rio dos Sinos (UNISINOS), São Leopoldo, 2010.
- [29] CASTRO, M.A.M., COSTA, F.G., BORBA, S.C., *et al.*, “Evaluation of physical and mechanical properties of soil-cement bricks formulated with steel co-products”, *Matéria UFRJ*, v. 21, n. 3, pp. 666–676, 2016. DOI:<https://doi.org/10.1590/S1517-707620160003.0064>
- [30] ALMEIDA, G.S.R., “*Gerenciamento de resíduos na indústria de construção civil: um estudo de caso*”, Trabalho de Conclusão de Curso (Engenharia de Produção), Universidade Tecnológica Federal do Paraná, Medianeira, 2014.
- [31] SUDARSHAN, N.M., RAO, T.C., “Experimental investigations on tensile strength behavior and microstructure of ultra-high performance fiber-based concrete”, *Research Article SN Applied Sciences*, v. 1, n. 3, pp. 215, 2019. DOI: <http://dx.doi.org/10.1007/s42452-019-0186-0>.
- [32] ROMERO, S.L., “*Precast prestressed concrete*”, Universidad Politécnica de Cartagena, Escuela de Arquitectura e Ingeniería de Edificación, Arquitectura Técnica, Cartagena, Espanha, 2012.
- [33] STORCH, I.S., DOBELIN, J.G.S., BATALHA, L.C., *et al.*, “Self- supporting tests in lattice joists subject to negative bending”, *Ibracon Structures and Materials Journal*, v. 10, n. 6, p. 1366–1395, 2017. DOI: <http://dx.doi.org/10.1590/s1983-41952017000600011>
- [34] MIHLAYANLAR, E., DILMAÇ, S., GUNER, A., “Analysis of the effect of production process parameters and density of expanded polystyrene insulation boards on mechanical properties and thermal conductivity”, *Materials & Design*, v. 29, n. 2, pp. 344–352, 2008. DOI: <http://dx.doi.org/10.1016/j.matdes.2007.01.032>.
- [35] SULONG, N.H.R., MUSTAPA, S.A.S., RASHID, M.K.A., “Application of expanded polystyrene EPS in buildings and constructions: a review”, *Applied Polymer*, v. 36, n. 20, 2019. DOI: <http://dx.doi.org/10.1002/app.47529>.
- [36] LI, V.C., *Engineered cementitious composites (ECC): bendable concrete for sustainable and resilient infrastructure*, Berlin, Springer Nature, 2019. DOI: <http://dx.doi.org/10.1007/978-3-662-58438-5>.
- [37] CALLISTER JUNIOR, W.D., RETHWISCH, D.G., *Ciência e engenharia de materiais: uma introdução*, 9. ed., Rio de Janeiro, LTC, 2016.
- [38] FISHER, J.M., “Strengthening open-web steel joists”, *Engineering Journal American Institute of Steel Construction*, v. 42, n. 4, pp. 247–259, 2005.